Available online at www.sciencedirect.com

ScienceDirect

Geochimica et Cosmochimica Acta 169 (2015) 30–44

Geochimica et Cosmochimica Acta

www.elsevier.com/locate/gca

Cell surface reactivity of *Synechococcus* sp. PCC 7002: Implications for metal sorption from seawater

Yuxia Liu [a,b], D.S. Alessi [b], G.W. Owttrim [c], D.A. Petrash [b], A.M. Mloszewska [b], S.V. Lalonde [d], R.E. Martinez [e], Qixing Zhou [a,*], K.O. Konhauser [b,*]

[a] *College of Environmental Science & Engineering, Nankai University, Tianjin 300071, China*
[b] *Department of Earth & Atmospheric Sciences, University of Alberta, Edmonton, Alberta T6G 2E3, Canada*
[c] *Department of Biological Sciences, University of Alberta, Edmonton, Alberta T6G 2E9, Canada*
[d] *UMR6538 Domaines Océaniques, CNRS-Université de Bretagne Occidentale, Institut Universitaire Européen de la Mer, 29280 Plouzané, France*
[e] *Institut für Geo- und Umweltnaturwissenschaften, Mineralogie-Petrologie Albert-Ludwigs-Universität, 79104 Freiburg, Germany*

Received 13 July 2014; accepted in revised form 21 July 2015; Available online 29 July 2015

Abstract

The past two decades have seen a significant advancement in our understanding of bacterial surface chemistry and the ability of microbes to bind metals from aqueous solutions. Much of this work has been aimed at benthic, mat-forming species in an effort to model the mechanisms by which microbes may exert control over metal contaminant transport in soils and groundwater. However, there is a distinct paucity of information pertaining to the surface chemistry of marine planktonic species, and their ability to bind trace metals from the ocean's photic zone. To this end, the surface properties of the cyanobacterium *Synechococcus* sp. PCC 7002 were studied as this genus is one of the dominant marine phytoplankton, and as such, contributes significantly to metal cycling in the ocean's photic zone. Zeta potential measurement indicates that the cell surfaces display a net negative charge. This was supported by potentiometric titration and Fourier transform infrared spectroscopy analyses demonstrating that the cells are dominated by surface proton releasing ligands, including carboxyl, phosphoryl and amino functional groups, with a total ligand density of 34.18 ± 1.62 mmol/g (dry biomass). Cd adsorption experiments further reveal that carboxyl groups play a primary role in metal adsorption, with 1.0 g of dry biomass binding an equivalent of 7.05×10^{-5} M of Cd from solution at pH = 8. To put this value into context, in 1 L of seawater, and with an open-ocean population of *Synechococcus* of 10^5 cells/mL in the photic zone, approximately 10 nmol of Cd could potentially be adsorbed by the cyanobacteria; an amount equivalent to seawater Cd concentrations. Although we have only focused on one microbial species and one metal cation, and we have not considered trace element assimilation, our results highlight the potential role of surface sorption by phytoplankton in the cycling of metals in the ocean.

1. INTRODUCTION

Bacterial surfaces possess abundant reactive ligands, such as carboxyl, hydroxyl, phosphoryl, and amino groups, that can deprotonate with increasing pH and are capable of binding metal cations (Fein et al., 1997; Cox et al., 1999). Those cations may then serve as sites for the nucleation of authigenic mineral phases (e.g., Clarke et al., 1997;

* Corresponding authors. Tel.: +86 (022) 23507800; fax: +86 (022) 66229562 (Q. Zhou). Tel.: +1 (780) 4922571; fax: +1 (780) 4922030 (K.O. Konhauser).
E-mail addresses: zhouqx@nankai.edu.cn (Q. Zhou), kurtk@ualberta.ca (K.O. Konhauser).

http://dx.doi.org/10.1016/j.gca.2015.07.033
0016-7037/

Konhauser et al., 1998). Recently, a number of studies have modeled the proton binding and charge properties of bacterial surfaces to determine the types and abundances of these reactive constituents and the capacity of bacteria to adsorb cations under different environmental conditions (Martinez et al., 2004; Fein et al., 2005; Lalonde et al., 2007; Baker et al., 2010; Kenney and Fein, 2011). Other studies have focused on how microbial surface chemistry and the charge characteristics may influence the microorganism's hydrophobic and hydrophilic properties (Van Loosdrecht et al., 1987; Mozes et al., 1988; Ahimou et al., 2001), which in turn, affects the ability of a microbe to adhere to solid surfaces (Van Loosdrecht et al., 1987; Ong et al., 1999; Cao et al., 2011). The main motivation for these studies was to better understand the mechanisms by which microbes might inhibit the transport of metal contaminants in the subsurface, and thus, to design effective bioremediation strategies (Bethke and Brady, 2000; Konhauser, 2007).

In the past decade, the database pertaining to cell surface reactivity has increased significantly (Mishra et al., 2010; Kenney and Fein, 2011; Wei et al., 2011). Yet to our knowledge such studies are limited with regards to cyanobacteria, in particular the determination of the organic ligands which contribute to cellular surface charge (Phoenix et al., 2002; Dittrich and Sibler, 2005, 2006; Lalonde et al., 2007; Pokrovsky et al., 2008; Hadjoudja et al., 2010) and their role in metal complexation (Benning et al., 2004; Yee et al., 2004; Pokrovsky et al., 2008; Acharya et al., 2009, 2012, 2013; Acharya and Apte, 2013). This is somewhat perplexing given that cyanobacteria are found in many terrestrial and aquatic habitats, and as primary producers and nitrogen fixers, they comprise the base of the food chain.

Cyanobacteria can grow either planktonically or benthically, and as such, the different species must have the means to alter their hydrophobic and hydrophilic properties. In this regard, studies have only recently begun characterizing the surface reactivity of cyanobacteria growing as freshwater mats or within hot spring sinters (Phoenix et al., 2002; Dittrich and Sibler, 2005; Lalonde et al., 2007). For instance, Phoenix et al. (2002) showed that the cell surface reactivity of *Calothrix* sp. strain KC97 can be described as a dual layer composed of a highly anionic cell wall enclosed within a neutrally-charged sheath. Interestingly, the dual-layered distribution of reactive sites on *Calothrix* sp. has several important ecophysiological implications, one of them being that the cyanobacterial sheath provides a protective mechanism against detrimental biomineralization (Phoenix et al., 2000). In the case of silicification in hot springs, this exopolymer was demonstrated to act as a filter against colloidal silica by restricting precipitation onto the sheath's outer surface and preventing silicification of the cell wall. Moreover, because *Calothrix* sp. strain KC97 is a benthic cyanobacterium that inhabits biofilms covering the silica sinters at hot springs, the ability of this microorganism to adhere to a mineral substratum is fundamental at preventing rapid removal from the hot spring site by the relatively fast-flowing discharge waters. In this regard, studies have suggested that bacterial adhesion is proportional to the microorganism's hydrophobicity and inversely proportional to the bacterium's surface charge (e.g., Van Loosdrecht et al., 1987).

By contrast, a study of various cyanobacteria by Fattom and Shilo (1984) demonstrated that planktonic cyanobacteria exhibit hydrophilic characteristics. The suggestion that an enclosing sheath of low electronegativity is important in inducing hydrophobicity (and thus encouraging surface adhesion) is corroborated by observations that the free-swimming hormogonia produced by benthic cyanobacteria are all hydrophilic in nature (Fattom and Shilo, 1984). Filaments in this planktonic, transient phase lack extracellular sheaths, thus exposing the highly electronegative cell walls. This, in turn, contributes significantly to the hormogonia's hydrophilic characteristic. Along similar lines, previous studies confirm that planktonic, *Synechococcus*-type cells (Dittrich and Sibler, 2005) and *Microcystis aeruginosa* (Hadjoudja et al., 2010) have low isoelectric points, giving those bacteria a highly negative surface charge and low hydrophobicity.

If planktonic species are hydrophilic, then it follows that those species will also be capable of reacting with polarized water molecules and dissolved metal cations. This has important ramifications for the oceans because the photic zone can be dominated by planktonic cyanobacteria, in particular, the genera *Synechococcus* and *Prochlorococcus*. For instance, *Synechococcus* populations vary from 10^4 to 10^5 cells/mL within the photic zone in the relatively rich waters of the Arabian Sea and off the coast of Peru (Waterbury et al., 1979; Worden et al., 2004), while Flombaum et al. (2013) predicted that the average contribution of *Synechococcus* and *Prochlorococcus* to ocean net primary production was 16.7% and 8.5%, respectively. Given their abundance in the oceans, understanding their surface reactivity towards cationic trace elements is critical to understanding the role that planktonic cyanobacteria play in trace metal sorption from the marine water column.

In this study, potentiometric titrations and modeling of cell surface reactivity were employed to constrain the acid dissociation constants (pK_a) and concentrations of proton-active sites that may bind metals to the cell surface of *Synechococcus* sp. PCC 7002, while zeta potential and Fourier transform infrared (FTIR) analyses were used to assess the surface chemical characteristics of the marine cyanobacterium. Cadmium adsorption experiments were also performed at various metal:bacterial site concentration ratios as a function of pH, to determine cyanobacterial efficiency at adsorbing Cd from solution, and by extension, other trace metal cations. Cd was specifically chosen in our study versus other metal cations for the following reasons: (1) Cd remains largely soluble at seawater pH; (2) its use in laboratory settings is not complicated by the precipitation of cadmium carbonate or hydroxide solids at our experimental conditions; (3) to facilitate comparison with other metal adsorption studies involving humic acids and other bacterial species where Cd is the usual metal chosen (Borrok et al., 2004a,b; Yee et al., 2004; Johnson et al., 2007; Ueshima et al., 2008; Alessi and Fein, 2010; Lalonde et al., 2010; Kenney and Fein, 2011; Petrash et al., 2011); and (4) for relevance to estuaries and other near-shore waters where Cd concentrations may be elevated (Petersen et al., 1998).

2. EXPERIMENTAL PROCEDURES

2.1. Bacterial growth

Axenic cultures of the cyanobacterial strain *Synechococcus* sp. PCC 7002 (henceforth referred to as *Synechococcus*) were grown at 30 °C in media A (Stevens and Van Baalen, 1973) supplemented with 0.01 M $NaNO_3$ (designated A+ media; Stevens and Porter, 1980) and buffered with 1 M Tris at pH 8.2. Sufficient biomass for potentiometric titrations or Cd adsorptions was obtained by using three 300 mL cultures, inoculated from the same starting culture, and each grown in 1 L Erlenmeyer flasks. Aeration was provided by constant shaking at 150 rpm and bubbling with humidified air. Growth was monitored by optical density measurements at 750 nm, and cells were harvested at late exponential phase ($OD_{750} = 0.58 \pm 0.03$) by centrifugation at room temperature (14,500 g, 10 min). Cells were subsequently washed four times in 30 mL of 0.01 M $NaNO_3$ electrolyte solution, incubated for 10 min between washes.

2.2. Transmission/scanning electron microscopy (TEM/SEM)

Cells were fixed in 2.5% gluteraldehyde-2% paraformaldehyde for 4 h at 4 °C, and washed 3 times in 0.1 M phosphate buffer saline (PBS, pH 7.2). For TEM imaging, fixed samples were stained with 1% osmium tetroxide (OsO_4 in 0.12 M cacodylate buffer, pH 7.2) for 1 h, washed in 0.1 M PBS, and dehydrated through a graded ethanol series (15 min in each 50%, 70%, 90% and 100% solution). Dehydrated tissue was impregnated with low-viscosity Spurr resin and cured for 24 h at 80 °C. 60 nm-thick sections were cut using a Reichert-Jung Ultramicrotome, mounted onto Formvarcarbon-coated, 200-mesh, copper grids, and stained with 2% uranyl acetate. A Philips FEI Morgagni 268 Transmission electron microscope (operating at 80 kV) was used to image the samples.

For SEM imaging, cells were fixed and dehydrated as described above. Dehydrated cells were dried in a desiccation chamber overnight, placed on aluminum SEM stubs, sputter coated with gold and imaged on a Philips FEI XL30 Scanning Electron Microscope operating at 20 kV.

2.3. Fourier transform infrared (FTIR) spectroscopy

FTIR spectroscopy was used to elucidate the composition of the functional groups exposed on the *Synechococcus* cells. Immediately after harvesting, cells were oven dried at 60 °C for 24 h, and then mixed with KBr powder (1:50, wt/wt) and pressed into a pellet. Pellets were then examined for FTIR spectra using a Deuterated Tri Glycine Sulfate (DTGS) detector attached to a Thermo Nicolet FTIR Spectrometer 8700. Infrared spectra were recorded over the range of 4000–500 cm^{-1} in absorbance mode and then converted into transmittance. For each averaged spectrum, 128 scans were collected at a resolution of 4 cm^{-1}. Background correction was performed by subtracting an air-only spectrum from the *Synechococcus* spectra.

2.4. Zeta potential measurements

Zeta potential measurements were performed to assess the net surface charge characteristics of *Synechococcus* cells, and conducted as described by Phoenix et al. (2002). Microbial cells were harvested, washed, and suspended in 0.01 M $NaNO_3$. pH was adjusted by adding small aliquots of HNO_3 (0.016, 0.16 and 1.6 M) or NaOH (0.019, 0.19 and 1.9 M) and stirring until the pH stabilized. Zeta potential analyses were performed using a Malvern Instruments Zetasizer Nano Series instrument. Bacteria-free 0.01 M $NaNO_3$ solutions were used as controls. An average of 10 readings for 3 biological replicates was collected. The average values ±1 standard deviations are reported here.

2.5. Potentiometric titrations

Potentiometric titrations were conducted as per Petrash et al. (2011). Plasticware and glassware used for solution preparation and potentiometric titrations were soaked in 10% nitric acid for 24 h, rinsed with 18 MΩ water repeatedly, and subsequently soaked in 18 MΩ water for 48 h. Before each titration, 0.5–0.7 g of biomass (wet weight) was re-suspended in ~50 mL of electrolyte solution (either 0.01 M $NaNO_3$, 0.56 M $NaNO_3$, or 0.56 M NaCl). A double-junction glass pH electrode (Orion ROSS ultra, filled with 3 M KCl) was calibrated using commercial pH buffers (Thermo Fisher Scientific; pH 2.0, 3.0, 4.0, 7.0, 10.0). The pH electrode was mounted into flasks containing the prepared alkalimetric titration solutions along with a magnetic stir bar, titrant dispenser, thermocouple, and Argon (Ar) gas line with a diffusion bubble stone. Solutions were acidified to pH ~3.0 with 2 M HCl, sealed with Parafilm, and purged with Ar for 30 min prior to, and throughout titrations, to maintain a CO_2-free atmosphere in the flask. Titrations were carried out a minimum of three times for each condition using separate batches of bacterial cultures. Blank titrations were performed for machine calibration, using bacteria-free 0.01 M $NaNO_3$, 0.56 M $NaNO_3$ and 0.56 M NaCl solutions.

Titrations were performed alkalimetrically from pH ~3.0 to 11.1 using a Man-Tech Associates QC-Titrate autotitrator which variably delivered CO_2-free 0.01 M NaOH in 0.1 pH increments, with an average equilibration time between additions of ~30 s. The volume of base added and corresponding pH changes were recorded at each titration step. Each addition of base occurred only after a pH electrode stability of 0.1 mV/s was attained, for a typical total titration time of ~50 min. Once pH ~11 was achieved, reverse 'down-pH' titrations were performed, decreasing the suspension to pH 3 with aliquots of 0.01 M HCl in order to test the reversibility of proton binding on the cells. Cellular integrity was assessed before, and after, the titrations by autofluorescence using a Zeiss Axioskop 2 epifluorescence light microscope. Cells that lysed may appear intact, but they do not display autofluorescence and so the microscopy would detect this lysis. No significant change in the relative abundance of cells that displayed autofluorescence was noted after the titration procedure. Immediately following titration, biomass was filtered onto

preweighed Whatman GF/C #42 filters (0.45 μm) and oven dried at 65 °C for 48 h for dry weight determination. The increased dry weight resulting from dried sea salt associated with the 0.56 M $NaNO_3$ and NaCl solutions was accounted for in our calculations so that the same weight of biomass was used in both the 0.56 M and 0.01 M ionic strength experiments.

To determine the acidity constants and concentrations of proton active functional groups on the bacterial surface, a non-electrostatic surface complexation model was chosen to fit the potentiometric titration data, using (1) linear programming as implemented in MATLAB (Lalonde et al., 2008a,b; Lalonde et al., 2010) to optimize ligand densities at every possible point in a fixed pK_a interval (in this case, 4–10 in 0.2 increments), and (2) least-squares optimization as implemented in FITEQL 4.0 (Herbelin and Westall, 1999) to describe, for a predetermined number of ligands, acidity constants (expressed as pK_a, equivalent to $-\log K_a$) and ligand densities that best describe the excess charge data (in this case, a three-site model adequately describes the data; see variance, or $V(Y)$, values in Table S1).

The charge balance in each titration step was calculated by the following charge balance equation:

$$[C_a - C_b] = [-Q] + [H^+] - [OH^-] \quad (1)$$

where $[C_a - C_b]$ is the concentration of acid added minus the concentration of base added; $[H^+]$ and $[OH^-]$ are the concentrations of proton and hydroxyl ions, respectively, and $[-Q]$ is the negative charge excess owing to deprotonation of bacterial ligands in solution, normalized to per gram of biomass.

2.6. Cadmium adsorption experiments

Batch Cd(II) adsorption experiments were conducted by measuring the change in aqueous Cd concentration that occurred upon exposure of a Cd solution to washed *Synechococcus* cells, following the methods of Kenney and Fein (2011). Three Cd concentrations (8.9×10^{-6} M, 8.9×10^{-5} M and 2.2×10^{-4} M) were tested for Cd adsorption in 0.01 M ionic strength. Cd adsorption at 0.56 M ionic strength was tested at a Cd concentration of 8.9×10^{-6} M. In all cases, a 1000 ppm Cd(II) commercial standard solution (Thermo Fisher Scientific) was diluted as needed in a matrix-matched solution (of either 0.01 M $NaNO_3$, 0.56 M $NaNO_3$ or 0.56 M NaCl) to prepare the appropriate Cd stock solution. The pH of Cd-bearing parent solutions was acidified to ~3.0 to prevent potential long-term precipitation of Cd from these solutions. A pellet of washed cells was suspended in the specific Cd-bearing solution to achieve a bacterial concentration of 10 g/L wet weight in each experiment. Aliquots (10 mL) were adjusted to the starting pH (between pH 3 and 9, in 1 pH unit intervals) using HNO_3 (0.016, 0.16 and 1.6 M) or NaOH (0.019, 0.19 and 1.9 M). The systems were mixed via end-over-end rotation at 40 rpm for 24 h to allow time for equilibration between the Cd and the cells, after which the final pH was measured. Cells were separated from solution by centrifugation at 14,500 g and filtration of the resulting supernatant through a 0.22 μm nylon membrane. The concentration of dissolved Cd remaining in the filtered supernatants was measured using an Inductively Coupled Plasma-Optical Emission Spectrometer (ICP-OES), calibrated with matrix-matched standards (Thermo Fisher Scientific). The concentration of Cd adsorbed to the cells was calculated as the difference between the initial and final Cd solution concentrations. Control experiments were conducted without bacteria to determine if Cd was lost to the experimental apparatus or by precipitation in the timeframe of the adsorption experiments. The analytical uncertainty of the ICP-OES for measuring Cd at experimental concentrations was determined to be ±2% by repeat analysis of standards. Experiments were conducted in triplicate for each Cd concentration, using three independent cultures.

Cd activities were determined based on the following hypothesized surface adsorption reactions:

$$R - L_n^- + Cd^{2+} \leftrightarrow R - L_nCd^+ \quad (2)$$

Best-fit equilibrium constants for Cd(II)-bacteria complexes were calculated using least-squares optimization as implemented in FITEQL (Herbelin and Westall, 1999). Cd-ligand stability constants are defined as:

$$K_{L_n-Cd^+} = \frac{[R - L_n - Cd^+]}{[R - L_n^-] \cdot a_{Cd^{2+}}} \quad (3)$$

where $[R - L_n - Cd^+]$ is the concentration of the Cd-ligand organic complex, $[R - L_n^-]$ is the concentration of ligands and $a_{Cd^{2+}}$ is the activity of Cd^{2+} in solution. The equilibrium constant, $K_{L_n-Cd^+}$ is reported as log $K_{L_n-\ Cd^+}$ for triplicate experiments. Calculations considered 6 aqueous Cd hydrolysis reactions and 3 cadmium carbonate complexes (Table S2; Baes and Mesmer, 1976; Stipp et al., 1993), and for systems where 0.56 M NaCl was the background electrolyte, aqueous cadmium chloride complexes (Table S2; Zirino and Yamamoto, 1972).

The reversibility of Cd adsorption behavior was also tested in our experiments. The Cd-loaded cells at 8.9×10^{-6} M Cd concentration, and at 0.01 M $NaNO_3$, 0.56 M $NaNO_3$ and NaCl ionic strengths were harvested, rinsed and re-suspended with corresponding $NaNO_3$ or NaCl solutions. The pH of the suspensions was adjusted to 3.0 by HNO_3 in order to desorb surface-bound Cd^{2+} from the cells (Urrutia and Beveridge, 1993; Yee and Fein, 2001). After being gently agitated for 24 h, the suspensions were centrifuged and filtered as previously described, and the Cd concentration in the supernatant was measured. The amount of Cd measured was compared to the concentration of Cd adsorbed to calculate the percent of Cd recovered.

3. RESULTS

3.1. TEM and SEM

Fig. 1 shows that *Synechococcus* sp. PCC 7002 is a small (<1 μm in diameter), sheathless, coccoid cyanobacterium, where the outer membrane acts as a semipermeable barrier toward molecules from the external environment. The internal structure is consistent with other cyanobacteria,

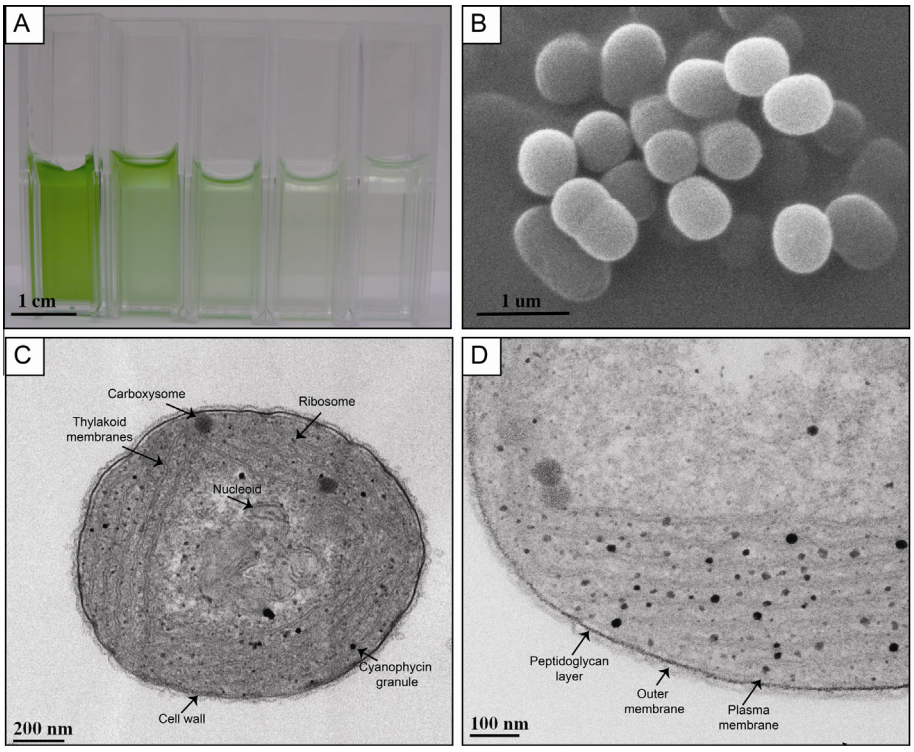

Fig. 1. (A) Samples of *Synechococcus* sp. PCC 7002 liquid cultures in A+ media, grown under constant illumination at 30 °C, and shown here at various densities, from 12×10^7 cells/mL (far left) to 0.9×10^7 cells/mL (far right). (B) SEM image of *Synechococcus* sp. PCC 7002 cells fixed with 2.5% gluteraldehyde, 2% paraformaldehyde and gold coated. (C) TEM image of ultrathin sections showing the ultrastructure of a representative *Synechococcus* sp. PCC 7002 cell taken at mid-logarithmic growth phase. (D) TEM image showing a close up of the cell wall, emphasizing the lack of a sheath.

containing cyanophycin granules, ribosomes, carboxysomes, thylakoids and a nucleoid region.

3.2. FTIR spectra

The functional groups and corresponding infrared spectra collected for *Synechococcus* are summarized in Fig. 2 and Table 1. Duplicate spectra from an individual culture, and spectra from two different batches of culture (4 total spectra) were identical, and so a representative spectrum is shown in Fig. 2. The amide I and amide II groups display absorption maxima at approximately 1655 cm^{-1} (C=O stretching) and 1534 cm^{-1}, respectively. These two ligands are characteristic of cyanobacterial outer membranes containing lipopolysaccharides and proteins (Benning et al., 2004; Jiang et al., 2004; Dittrich and Sibler, 2006). Strong

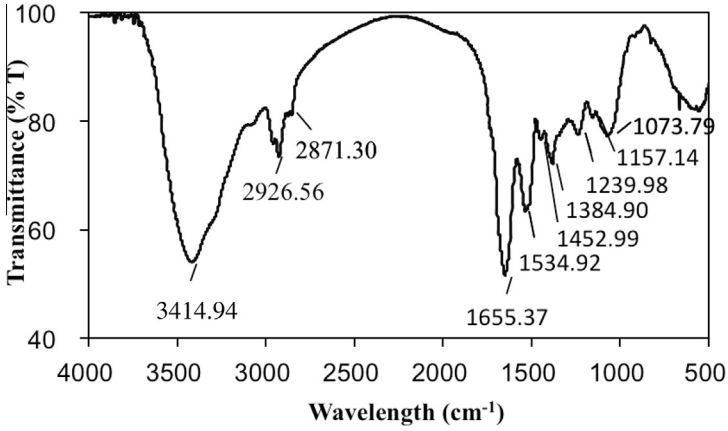

Fig. 2. FTIR transmittance spectrum of *Synechococcus* sp. PCC 7002 cells at mid-logarithmic growth phase.

Table 1
Summary of proposed functional groups and corresponding infrared wavelengths.

IR band	Wavelength (cm^{-1})	Functional group assignment
1	3415	Antisymmetric stretching of O–H vibrations in water (Peng et al., 2003)
2	3000–2800	Stretching of C–H, $–CH_3$, and $>CH_2$ functional groups (Yee et al., 2004)
3	1655	Stretching of C═O in amide I, associated with proteins (Benning et al., 2004; Jiang et al., 2004)
4	1534	N–H bending and C–N stretching in amide II, associated with proteins (Dittrich and Sibler, 2006; Petrash et al., 2011)
5	1470–1350	Deformation of C–H, $–CH_3$, and $>CH_2$ functional groups (Yee et al., 2004)
6	1239	Asymmetric stretching of PO_2^- associated with phosphodiesters and phosphate, vibrations of –COOH, and C–O–C group in esters (Yee et al., 2004; Petrash et al., 2011)
7	1200–900	Mixed vibrational modes of carbohydrates; C–O–C, C–O–P, P–O–P ring vibrations of polysaccharides (Yee et al., 2004; Leone et al., 2007)

absorption peaks at 2800–3000 cm^{-1} and 1470–1350 cm^{-1} are tentatively assigned to C–H stretching vibration of $–CH_3$ and $>CH_2$ functional groups, which are attributed to the fatty acid components found in membrane phospholipids (Yee et al., 2004). Peaks representing >P═O double-bond asymmetric stretching are present at 1239 cm^{-1}, and are characteristic of nucleic acid or phosphorylated polysaccharides (Yee et al., 2004), while the peaks between 1200 and 900 cm^{-1} are dominated by C–O–C, C–O–P and P–O–P stretching vibrations of lipopolysaccharides (Yee et al., 2004; Leone et al., 2007). Strong peaks at 3415 cm^{-1} are assigned to antisymmetric stretching of O–H vibrations in water (Peng et al., 2003).

3.3. Zeta potential

The charge at the *Synechococcus* cell surface was measured as a function of pH (Fig. 3). The zeta potential remains below −35 mV from pH 4 to 10, indicating that the cells continuously exhibit a net negative surface charge over the tested pH range. In particular, the cells display a sharp increase in electronegativity from pH 4 to 6, above which it remains constant, suggesting that maximum electronegativity occurs above pH 6.

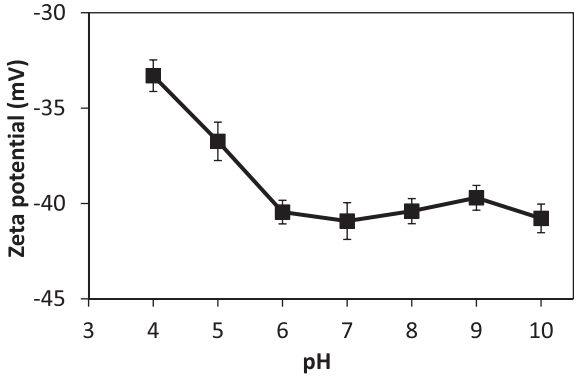

Fig. 3. Zeta potential measurements conducted using suspensions of *Synechococcus* sp. PCC 7002 cells incubated in 0.01 M $NaNO_3$ buffer as a function of pH. The average of three independent experiments is plotted. Error bars represent the ±1-sigma standard deviation of the averaged data sets.

3.4. Potentiometric titrations

3.4.1. Using 0.01 M $NaNO_3$ solutions

Fig. 4A shows titration data in 0.01 M $NaNO_3$ plotted in terms of mmol of deprotonated sites (or charge excess) per gram of bacteria dry mass. The slope at any given point can be interpreted as the instantaneous buffering capacity at that pH. That is, the slope indicates the rate of ligand deprotonation, per unit of pH. The titration data show that *Synechococcus* can significantly buffer pH over the entire pH range (4–10) of this study. Figure S1 is a representative example of titration reversibility for four replicates. The up-pH and down-pH titrations did not exhibit remarkable differences, suggesting reversibility of the proton adsorption/desorption reactions on the cell surface occur within the timescale of the experiments. The three-site model from FITEQL modeling yields variance, or $V(Y)$, values of $0.1 < V(Y) < 20$ (Table S1), indicating a good fit to the experimental data (Westall, 1982). These fits, combined with the FTIR measurements, suggest the presence of at least three types of proton-active ligands on the *Synechococcus* cell surface. The model site distributions are shown at Fig. 5A, with surface ligand acidity constants and concentrations of ligands presented in Table 2. Based on FTIR spectra and analogy in acidity constants with respect to known compounds, these ligands likely correspond to carboxyl (pK_a of 5.42 ± 0.03), phosphoryl (pK_a of 7.42 ± 0.03), and amino (pK_a of 9.95 ± 0.16) functional groups, respectively.

A summation of the ligand concentrations across the analyzed pH range reveals that *Synechococcus* exhibits an average total site density of 34.18 ± 1.62 mmol/g (dry weight) at 0.01 M ionic strength, corresponding to carboxyl, phosphoryl, and amino groups with surface densities of 12.78 ± 0.43, 6.55 ± 0.43, and 14.12 ± 1.34 mmol/g (dry weight), respectively (Fig. 5A).

3.4.2. Using 0.56 M $NaNO_3$ solutions

Fig. 4B shows cell titration data in 0.56 M $NaNO_3$ plotted in terms of mmol of deprotonated sites (or excess charge) per gram of bacteria dry mass. The three-site model calculated using FITEQL provides good fit to the experimental data (see $V(Y)$ values in Table S1). Similar to the 0.01 M $NaNO_3$ results, they likely correspond to carboxyl (pK_a of 5.10 ± 0.02), phosphoryl (pK_a of 7.20 ± 0.08),

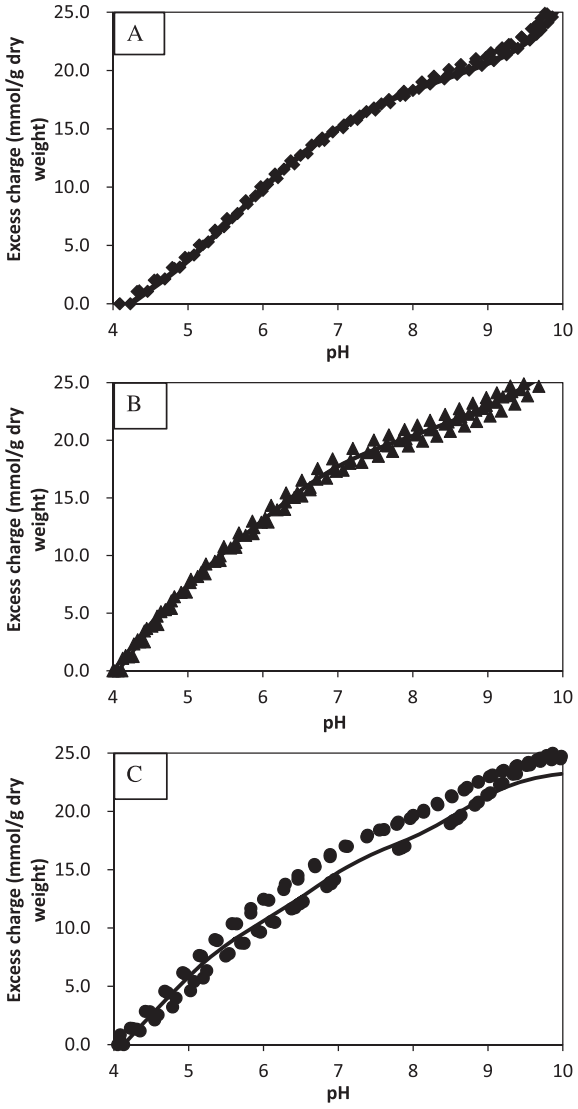

Fig. 4. Potentiometric titration data for *Synechococcus* sp. PCC 7002 cells in terms of excess charge as a function of pH, at three ionic strengths: (A) 0.01 M $NaNO_3$, (B) 0.56 M $NaNO_3$, (C) 0.56 M NaCl.

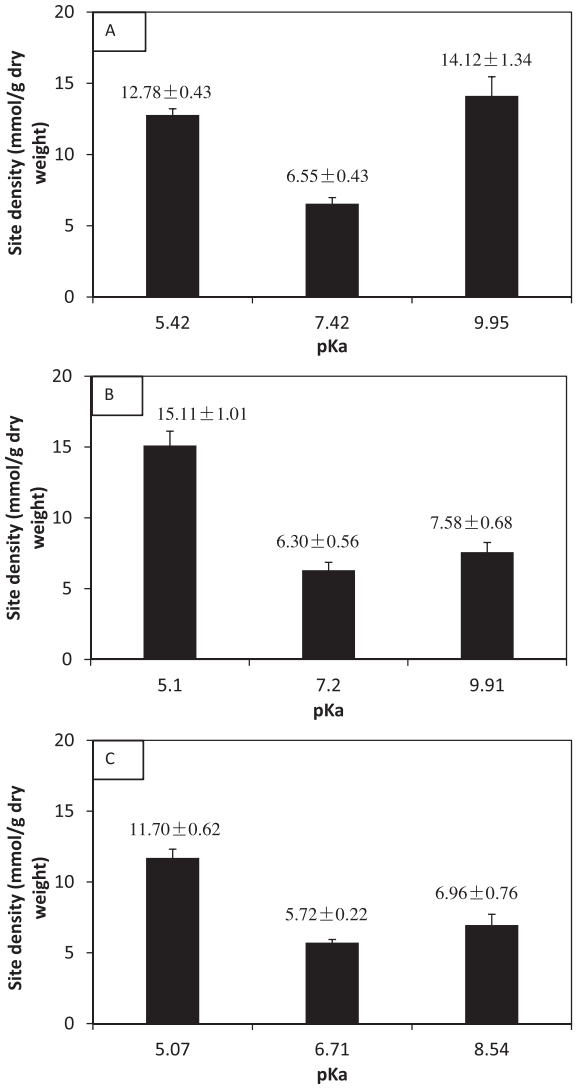

Fig. 5. Ligand densities of 3-pK_a titration models at ionic strengths of (A) 0.01 M $NaNO_3$, (B) 0.56 M $NaNO_3$, and (C) 0.56 M NaCl.

and amino (pK_a of 9.91 ± 0.25) groups, respectively. This suggests that the high ionic strength (0.56 M) did not greatly impact the cell wall functional group composition relative to the 0.01 M ionic strength condition.

A summation of the ligand concentrations across the analyzed pH range reveals that *Synechococcus* exhibits an average total site density of 28.99 ± 0.52 mmol/g (dry weight) in 0.56 M $NaNO_3$ ionic strength, corresponding to carboxyl, phosphoryl, and amino groups with surface densities of 15.11 ± 1.01, 6.30 ± 0.56, and 7.58 ± 0.68 mmol/g (dry weight), respectively (Fig. 5B). These modeling results demonstrate a slight decrease in total site density as a function of increasing ionic strength, with amino groups being the most impacted compared with 0.01 M ionic strength.

3.4.3. Using 0.56 M NaCl solutions

Fig. 4C shows titration data of *Synechococcus* cells titrated in 0.56 M NaCl plotted in terms of mmol of deprotonated sites (or charge excess) per gram of bacteria dry mass. A three-site surface complexation model provides a good fit to the experimental data (Table S1). Again, these functional groups likely correspond to carboxyl (pK_a of 5.07 ± 0.03), phosphoryl (pK_a of 6.71 ± 0.07), and amino (pK_a of 8.54 ± 0.15) groups, respectively. The titrations in 0.56 M NaCl show lower pK_a values than titrations in both 0.01 M $NaNO_3$ and 0.56 M $NaNO_3$. This is likely due to the differences in the ways that NO_3^- and Cl^-, which have hydrated ionic radii of 34 Å and 33 Å respectively and different affinities for solution Na^+, influence the electrical charge at the surface and ultimately the reactivity to protons in solution (Ntalikwa, 2007).

A summation of the ligand concentrations across the analyzed pH range reveals that *Synechococcus* exhibits an average total site density of 24.38 ± 0.64 mmol/g (dry

Table 2
Parameters obtained from best-fit, non-electrostatic proton adsorption models of titration data (pK_a and total density of ligand) and best-fit Cd-ligand stability constants ($-\log K_{CdL}$) for *Synechococcus* sp. PCC 7002.

Ionic strength	Ligand class	Average pK_a	Mean L_T (mmol g^{-1})	Functional group	log K_{CdL}		
					1 ppm	10 ppm	25 ppm
0.01 M $NaNO_3$	A	5.42 ± 0.03	12.78 ± 0.43	Carboxyl	2.54 ± 0.24	2.61 ± 0.17	2.88 ± 0.16
	B	7.42 ± 0.03	6.55 ± 0.43	Phosphoryl		4.92 ± 0.10	5.34 ± 0.20
	C	9.95 ± 0.16	14.12 ± 1.34	Amino			6.61 ± 0.22
0.56 M $NaNO_3$	A	5.10 ± 0.02	15.11 ± 1.01	Carboxyl	2.33 ± 0.36		
	B	7.20 ± 0.08	6.30 ± 0.56	Phosphoryl	4.25 ± 0.22		
	C	9.91 ± 0.25	7.58 ± 0.68	Amino			
0.56 M NaCl	A	5.07 ± 0.03	11.70 ± 0.62	Carboxyl	1.15 ± 0.67		
	B	6.71 ± 0.07	5.72 ± 0.22	Phosphoryl	1.78 ± 0.07		
	C	8.54 ± 0.15	6.96 ± 0.76	Amino	2.74 ± 0.03		

weight) in 0.56 M NaCl, corresponding to carboxyl, phosphoryl, and amino groups with surface densities of 11.70 ± 0.62, 5.72 ± 0.22, and 6.96 ± 0.76 mmol/g (dry weight), respectively (Fig. 5C). These site concentrations are similar to those found in the 0.56 M $NaNO_3$ electrolyte, and lower than those in 0.01 M $NaNO_3$ electrolyte.

3.5. Cadmium adsorption

3.5.1. Using 0.01 M $NaNO_3$ solutions

The pH dependence of *Synechococcus*-metal sorption in 0.01 M $NaNO_3$ is depicted in Fig. 6. Cd sorption edges were determined at 8.9×10^{-6} M (Fig. 6A), 8.9×10^{-5} M (Fig. 6B) and 2.2×10^{-4} M (Fig. 6C). Experimental Cd adsorption data were modeled with FITEQL, using the average *Synechococcus* site concentrations and their acidity constants calculated from potentiometric titrations. Data between pH 3.0 and 8.5 were modeled to calculate Cd mass action (K) constants, as appreciable loss of Cd due to the precipitation of cadmium carbonate solids was apparent at higher pH (Figs. 6 and S2). As depicted in Table 2, Cd adsorption behavior was fit using surface complexation models that invoke between 1 and 3 distinct sites. For low Cd concentrations, an excellent fit was achieved when only carboxyl sites participated in Cd adsorption (Fig. 6A); the Cd-ligand stability constant (as log K_{Cd}) determined for the carboxyl moieties is 2.54 ± 0.24. At higher initial Cd concentrations (8.9×10^{-5} M), a two-site model provides the best fit (Fig. 6B), and the Cd-ligand stability constants (as log K_{Cd} values) correspond to carboxyl and phosphoryl groups are 2.61 ± 0.17 and 4.92 ± 0.22, respectively. At the highest Cd concentration (2.2×10^{-4} M), it was necessary to invoke both carboxyl and phosphoryl sites to explain Cd adsorption behavior (Fig. 6C). However, it is likely that amino functional groups are involved in binding Cd^{2+} from solution at higher pH, as a three-site model including amino groups (log $K_{Cd} = 6.61 \pm 0.22$) did provide an improved fit.

As shown in Fig. 6, we observe a positive correlation between Cd removed from solution and pH, and a negative correlation between Cd removed and the initial Cd concentration. In experiments with low Cd concentrations (8.9×10^{-6} M, Fig. 6A), nearly 100% removal occurs at pH < 6; at higher pH, a plateau in the adsorption edge is observed. A decrease in Cd removal from solution is observed when Cd is gradually increased, suggesting that the functional groups are becoming saturated. At 8.9×10^{-5} M, 80% of the Cd is removed, with a corresponding plateau shifted to above pH 7 (Fig. 6B), whereas at 2.2×10^{-4} M Cd, less than 70% is removed and no plateau is observed over the pH range studied (Fig. 6C).

3.5.2. Using 0.56 M $NaNO_3$ solutions

The pH dependence of *Synechococcus*-metal sorption in 0.56 M $NaNO_3$ is depicted in Fig. 6D. Cd sorption edges were determined at the lowest total Cd concentration in this study, 8.9×10^{-6} M, because higher bacteria:metal ratios are more representative of natural conditions, i.e., total Cd in seawater is $<8 \times 10^{-9}$ M. A two-site model (invoking carboxyl and phosphoryl sites) fits the Cd sorption data well (log K_{Cd} values corresponding to carboxyl and phosphoryl groups are 2.33 ± 0.36 and 4.25 ± 0.22, respectively; Table 2).

The positions of the adsorption edges conducted at ionic strengths of 0.01 M and 0.56 M $NaNO_3$ are different (Fig. 6A and D). For example, 50% Cd uptake occurs at pH ~5 at 0.01 M, while it occurs at pH ~6 in the 0.56 M electrolyte. This is likely due to the increased competition of Na^+ with Cd^{2+} for adsorption onto bacterial surface functional groups (Alessi et al., 2010), or from abacterial surface perspective, the mitigation of the electric field near the surface due to increased ion shielding at higher ionic strengths. However, the final extent of Cd adsorption at higher pH relevant to marine systems (pH = 8) was roughly similar (nearly 100% removal was observed with increasing pH, Fig. 6D).

3.5.3. Using 0.56 M NaCl solutions

The pH dependence of *Synechococcus*-metal sorption in 0.56 M NaCl and at 8.9×10^{-6} M Cd is depicted in Fig. 6E. A three-site model that includes carboxyl, phosphoryl, and amino sites and considers aqueous cadmium chloride complexes (see Table S2 and Figure S3) provides an excellent fit; Cd-ligand stability constants were 1.15 ± 0.67 (carboxyl),

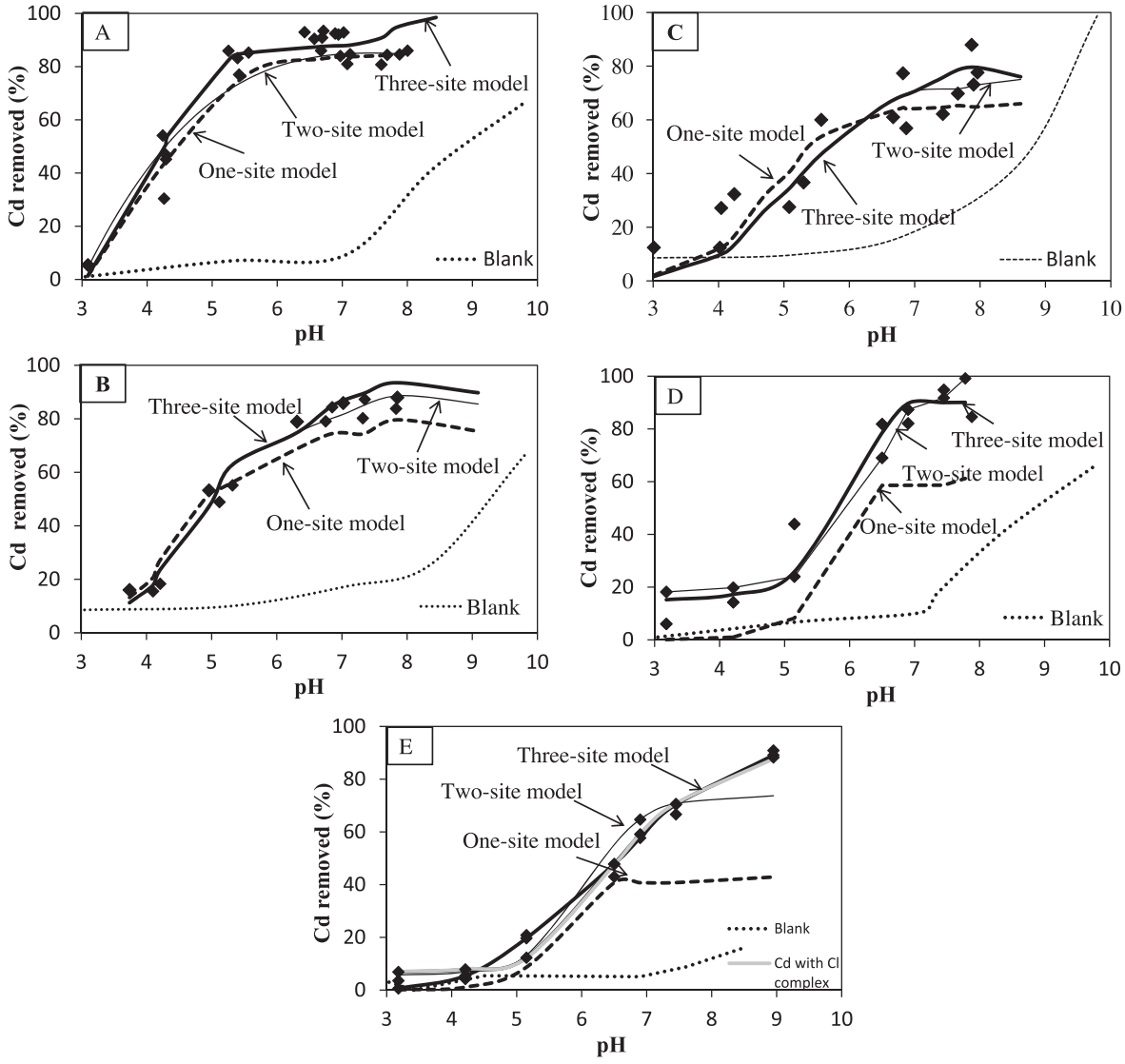

Fig. 6. Cd adsorption edges for *Synechococcus* sp. PCC 7002 cells exposed to 0.01 M $NaNO_3$ ionic strength at three different Cd concentrations: (A) 8.9×10^{-6} M; (B) 8.9×10^{-5} M; (C) 2.2×10^{-4} M; (D) 8.9×10^{-6} M Cd at 0.56 M $NaNO_3$ ionic strength; (E) 8.9×10^{-6} M Cd at 0.56 M NaCl ionic strength. The biomass concentration was 10 g/L (wet weight).

1.78 ± 0.07 (phosphoryl), and 2.74 ± 0.03 (amino), respectively.

The position of the Cd adsorption edge in 0.56 M NaCl shifted to the left compared to the 0.01 M and 0.56 M $NaNO_3$ electrolyte, for reasons explained previously. The point of 50% Cd uptake occurs at pH ~6.5, a full 1.5 pH units higher than in 0.01 M $NaNO_3$ and 0.5 pH units higher than in 0.56 M $NaNO_3$. These results suggest that the ionic strength and the type of anion present affect the Cd adsorption behavior. Nonetheless, the final extent of Cd adsorption at higher pH relevant to marine systems (pH = 8) was roughly similar (100% removal), implying that *Synechococcus* cells can remove most of the Cd^{2+} from the low Cd concentration solutions.

3.5.4. Testing the reversibility of cadmium adsorption

Reversibility of Cd^{2+} sorption to *Synechococcus* cells was tested by lowering the pH of bacteria-metal suspensions to pH 3 using 2 M HNO_3. At pH 3, less than 15% of the 8.9×10^{-6} M cadmium in the system should be adsorbed to the cells (see Fig. 6). More than 80% of the adsorbed Cd^{2+} was desorbed from the biosorbents. The missing recovery efficiency may be attributed to an intracellular metal diffusion process (absorption), or potentially, to a limited amount of biomass missing during the adsorption/desorption cycle. However, these cadmium desorption experiments confirm that the primary mechanism of metal removal from solution is reversible cadmium adsorption to *Synechococcus* cells.

4. DISCUSSION

4.1. Surface reactivity of planktonic *Synechococcus*

The primary aim of this study was to characterize the surface reactivity of the sheathless marine cyanobacterium, *Synechococcus* sp. PCC 7002, by evaluating the ability of organic ligands attached to its cell wall to adsorb metal cations. Since the surface charge of bacterial cells, in general, is established by proton dissociation from surface exposed ligands (Fein et al., 2005), the net electronegativity of *Synechococcus* cells provides evidence that those ligands are highly reactive for binding metal cations under our experimental conditions. The protonation state of cell surface ligands is strongly pH dependent; an increase in pH will cause ligands to systematically deprotonate to yield discrete anionic metal binding sites. As for most bacterial surfaces, at low pH (pH 4–6) the sites most responsible for deprotonation are carboxyl groups (reaction (4)). At circumneutral pH (pH 5–8) phosphoryl groups additionally deprotonate (reaction (5)), while at alkaline pH (pH 8–10) both amino groups (reaction (6)) and hydroxyl groups (reaction (7)) become increasingly important.

$$R-\mathrm{COOH}+\mathrm{OH}^- \rightarrow R-\mathrm{COO}^-+\mathrm{H_2O} \quad (4)$$

$$R-\mathrm{PO_4H_2}+\mathrm{OH}^- \rightarrow R-\mathrm{PO_4H}^-+\mathrm{H_2O} \quad (5)$$

$$R-\mathrm{NH_3^+}+\mathrm{OH}^- \rightarrow R-\mathrm{NH_2}+\mathrm{H_2O} \quad (6)$$

$$R-\mathrm{OH}+\mathrm{OH}^- \rightarrow R-\mathrm{O}^-+\mathrm{H_2O} \quad (7)$$

With regards to *Synechococcus* sp. PCC 7002, a decrease in surface charge associated with an increasing pH implies that carboxyl and phosphoryl groups become deprotonated to form negatively charged sites, and must occur more frequently than positively charged amino groups. The slight shift in the negative charge of a bacterial surface with increasing pH then implies deprotonation of amino groups, the former becoming electroneutral sites. Since we do not model potentiometric titration data above pH 10, we cannot be sure whether significant hydroxyl groups are also present. FTIR measurements and their analogy to acidity constants of known compounds, support our interpretation for the presence of both negatively charged carboxyl/phosphoryl groups and positively charged amino groups on the cell wall.

4.2. Comparisons with benthic cyanobacteria

Our potentiometric titration results are consistent, but not identical, with previous studies using planktonic species. For instance, to describe the proton binding of two strains of *Synechococcus*-type picoplankton, Dittrich and Sibler (2005) proposed 2 three-site models with the acidic sites attributed to carboxyl ($pK_a = 4.85$ and 4.98) and phosphoryl groups ($pK_a = 6.56$ and 6.69), and the alkaline sites attributed to amino groups ($pK_a = 8.76$ and 8.66). Lalonde et al. (2007) grouped the functional groups of natural cyanobacterial mats in Yellowstone National Park (USA) into three pK_a ranges of 4–6, 6–8, and 8–10, which corresponded to carboxyl, phosphoryl and amino groups, respectively. Composite titration data for intact filaments (including wall and sheath material) of the benthic cyanobacterial *Calothrix* sp. strain KC97 were determined to contain six functional groups ($pK_a = 5.02 \pm 0.25$, 5.70 ± 0.13, 6.23 ± 0.16, 7.34 ± 0.25, 8.13 ± 0.08 and 8.92 ± 0.23), whereas isolated sheaths contained five functional groups ($pK_a = 4.62 \pm 0.39$, 6.12 ± 0.14, 7.26 ± 0.22, 8.07 ± 0.11 and 9.15 ± 0.18) (Phoenix et al., 2002). Despite a similarity in functional group composition, the sheath's charge was almost equally dominated by low pH carboxyl groups and high pH amine groups, making a net surface charge that is close to neutral. By contrast, intact cells were dominated by carboxyl groups, yielding a more negative surface charge. Thus, the cell surface reactivity of *Calothrix* sp. strain KC97 can be described as a dual layer composed of a highly electronegative cell wall surrounded by an electroneutral sheath.

When considering the proton binding site density, our marine *Synechococcus* cells had on average an order of magnitude greater concentration (24.38–34.18 mmol/g dry mass) than the two fresh water cyanobacterial species (1.66 and 0.69 mmol/g dry mass) described by Dittrich and Sibler (2005), as well as *Calothrix* sp., whose cell surfaces had site densities of 0.08 mmol/g dry mass (Phoenix et al., 2002). They are of a similar magnitude to natural cyanobacterial mats whose cell surfaces had a site density of 6.12–19.23 mmol/g (dry mass) (Lalonde et al., 2007). It is not entirely clear to us why our pK_a values are somewhat higher than those reported in Dittrich and Sibler (2005). Several variables may account for this: (1) differences in the cell wall functionality and reactivity (Brahamsha, 1996; Claessens et al., 2004); (2) differing cell growth and washing protocols (Borrok et al., 2004b; Johnson et al., 2007; Ueshima et al., 2008; Alessi and Fein, 2010; Kenney and Fein, 2011); and (3) varying approaches to the titrations and modeling the data in a thermodynamic framework (e.g., Borrok et al., 2005; Fein, 2006; Alessi et al., 2010; Kapetas et al., 2011). In order to assess which of these variables are important, a systematic study controlling for these variables would be necessary; although such a study is outside of the scope of this manuscript which focuses on metal binding.

Collectively, these studies show that cyanobacteria display an overall net negative charge, but the magnitude depends on the surface structures present. For planktonic species, the absence of a sheath results in the anionic nature of the cell surfaces, increased hydrophilicity, and a greater potential to sorb trace metals from aqueous solutions. Conversely, benthic species produce extracellular layers, such as a sheath, that makes their surfaces more electroneutral, and in the case of those growing at hot springs, the increased hydrophobicity not only provides the cells with protection against detrimental biomineralization, but it enhances their adhesion to the underlying substrata (Phoenix et al., 2000, 2002).

4.3. Metal adsorption in the marine photic zone

Differences in metal adsorption were found to depend upon the relative proportion of biomass to dissolved metal. For instance, in the case of relatively high biomass:metal

Table 3
A literature compilation comparing the ability of various bacterial strains and natural consortia to adsorb Cd(II).

Bacterial type	Site density mmol g^{-1}	Adsorbed Cd Mol L^{-1}[e]	Reference
Purified alginate	1.73[a]	4.00×10^{-5}	Petrash et al. (2011)
Mucus lining of *Thelepus crispus*	11.26[a]	1.11×10^{-5}	Lalonde et al. (2010)
Pseudomonas putida	1.80[b]	4.89×10^{-5}	Ueshima et al. (2008)
Bacillus pseudofirmus	1.25[b]	7.56×10^{-5}	Kenney and Fein (2011)
Bacillus circulans	1.85[b]	7.56×10^{-5}	Kenney and Fein (2011)
Bacillus subtilis	1.39 [b]	4.45×10^{-5}	Alessi and Fein (2010)
Bacterial consortia[c]	1.90[b]	$(6.90–8.46) \times 10^{-5}$	Johnson et al. (2007)
Bacterial consortia[c]	1.10[b]	$(4.63–6.23) \times 10^{-5}$	Borrok et al. (2004a,b)
Bacterial consortia[d]	0.75–2.05[b]	$(6.67–8.45) \times 10^{-5}$	Borrok et al. (2004a,b)
Cyanobacterium *Calothrix*	1.46[a]	3.50×10^{-5} (pH ~6)	Yee et al. (2004)
Cyanobacterium *Synechococcus*	20.70 ± 0.65[a]	7.81×10^{-6}	This study (1 ppm)

[a] Site concentrations in mmol per dry mass.
[b] Site concentrations in mmol per dry mass converted from a wet-to-dry ratio of 5:1.
[c] Bacteria consortia grown from nature.
[d] Bacterial consortia grown from industrial wastes and contaminated soils.
[e] Average adsorbed concentration at pH ~8.

ratios (i.e., 8.9×10^{-5} M Cd experiments in 0.01 M electrolyte), we determined that 1.0 g dry biomass of *Synechococcus* cells (containing 34.18 ± 1.62 mmol/g dry mass of deprotonated ligands) can bind an equivalent of 7.05×10^{-5} M of Cd^{2+} (initial Cd concentration of 8.9×10^{-5} M, 0.01 M $NaNO_3$ electrolyte solution and pH = 8). These results fall within the range of a wide variety of bacteria (Table 3; Yee et al., 2004; Borrok et al., 2004b; Johnson et al., 2007; Pokrovsky et al., 2008; Alessi and Fein, 2010; Lalonde et al., 2010; Kenney and Fein, 2011; Petrash et al., 2011). This suggests that patterns of metal adsorption may not be species-specific when abundant biomass is present. Thus, a generalized model of proton and metal binding can provide reasonable estimates of adsorption behavior (Yee and Fein, 2001; Borrok et al., 2005). By contrast, when the biomass:metal ratios are low, 100% Cd sorption is not observed because there are not enough available ligands to adsorb all available dissolved Cd.

Irrespective of biomass:metal ratios, at seawater pH, deprotonated cyanobacterial carboxyl groups are most important for binding Cd, followed by phosphoryl sites. This is generally consistent with results of previous studies which demonstrate that cell surface carboxyl groups dominate Cd recovery near pH 8 across a wide range of bacterial species (Yee et al., 2004; Johnson et al., 2007; Pokrovsky et al., 2008; Kenney and Fein, 2011). The extent of Cd adsorption onto *Synechococcus* cells at pH ~8 exhibits no dependence upon salt concentration, though titrations of cells with different ionic strength conditions displayed slightly different buffering capacities, and apparent site densities (especially the amino groups) decreased slightly in response to increased salt concentration. The effect of ionic strength on *Synechococcus* cell surface characteristics is comparable to other Gram-negative bacteria species reported in the literature. For instance, Ledin et al. (1997) found that the extent of adsorption for metals onto *Pseudomonas putida* decreased with increasing ionic strength (0.01–0.1 M), but the magnitude of this decrease was relatively insignificant for some metals. Likewise, no significant differences were observed in the buffering capacity of *Shewanella putrefaciens* as the ionic strength increased from 0.02 to 0.1 M (Haas et al., 2001) or for *Aquabacterium commune* and *Gloeocapsa sp. f-6gl*as when ionic strength increased from 0.01 to 1.0 M (Ojeda et al., 2008; Pokrovsky et al., 2008).

Given that the average *Synechococcus* concentrations are 7.4×10^{10} cells/L (cell counts data on a haemocytometer, $OD_{750} = 0.320$ corresponding to 4.1×10^{10} cells/L, $OD_{750} = 0.580$ corresponding to 7.4×10^{10} cells/L), then a simple extrapolation suggests that each individual cell could potentially bind 10^{-16} mol (7.05×10^{-5} M divided by 7.4×10^{10} cells/L) of Cd to their cell surface. This of course is a variable amount because the cell surfaces will adsorb other metal cations from natural solutions due to competitive binding, most Cd in solution will be complexed by chloride (Figure S2E) or dissolved organic ligands, and some fraction of aqueous Cd would be expected to precipitate as cadmium carbonate solids at seawater conditions (pH ~8.3) (Stipp et al., 1993), as was observed in our Cd precipitation control experiments (Fig. 6E).

Due to the availability of proton-active functional groups on the cell surface, our data indicate that *Synechococcus* has the potential to play an important role in metal cycling – via adsorption – in the oceans. Unlike the dual-layered surface of *Calothrix* sp. (with sheath material contributing 15% of the total site density), which provides these cyanobacteria with a neutral surface to facilitate attachment to silica sinters (Phoenix et al., 2002), the highly anionic surface of *Synechococcus* binds metal cations from seawater. If one considers that an active bloom of *Synechococcus* may contain 10^4–10^5 cells/mL (Waterbury et al., 1979), then 10^{-9}–10^{-8} M of Cd, or 1–10 nM (10^4–10^5 cell/mL multiplied by 10^{-16} mol/cell of Cd) can be adsorbed by the cyanobacteria per 1 L of water column. Given that the total Cd in seawater is no more than 8×10^{-9} M, or 8 nM (Mart et al., 1982; Danielsson et al., 1985; de Baar et al., 1994; Pai and Chen, 1994), a

population of *Synechococcus* could theoretically adsorb all dissolved Cd from seawater in the photic zone, if equilibrium metal adsorption conditions were achieved.

Of course, this value is not meant to be taken literally as it does not consider a number of competing mechanisms, such as (1) Cd precipitation or binding by Cl^- anions, (2) Cd binding to organic ligands, and (3) competition for binding sites on the cyanobacteria by other metals. In the first instance, Cd adsorption behavior to cells can be impacted by the formation of $CdCO_3$ solids, and aqueous Cd-chloride complexes (predominantly $CdCl_2^0$ and $CdCl^+$) (Figure S3). In fact, it has been reported that 97.2% of dissolved inorganic Cd in seawater exists as chloride complexes (Byrne et al., 1988), consistent with our aqueous speciation modeling (Figure S2E).

In the second instance, Bruland (1992) suggested that 10% of the Cd presented in the upper 600 m of the central North Pacific is in the particulate fraction, while 90% is dissolved. Of the former, some of the particulate Cd likely includes microbial biomass (Sherrell and Boyle, 1992). Of the latter, 67% is bound to strong organic complexes at concentrations of only 0.1 nM; the remaining 33% comprises chloride complexes ($CdCl_2$ and $CdCl^+$). In Narragansett Bay, Rhode Island, 73–83% of dissolved Cd was organically complexed (Wells et al., 1998). This then leads to the question of whether those ligands are Cd-specific, i.e., with similar function to siderophores to increase the bioavailability of Fe (Neilands, 1995) or the organic exudates produced by algae to limit the toxicity of Cu (González-Dávila et al., 1995). Certainly, Cd is a particularly efficient metal for inducing production of metal-binding ligands in plankton (Ahner and Morel, 1995), with both field and experimental studies (e.g., Ahner et al., 1998; Dupont and Ahner, 2005) demonstrating that Cd binding ligands are produced far in excess of dissolved Cd concentrations.

In the third instance, it is well known that the propensity for an organic ligand to bind a divalent metal (i.e., their log K values) increases as we move from left to right in the periodic table, reaching a maximum with Cu^{2+}. This trend, called the "Irving-Williams Series", is observed with practically all oxygen- and nitrogen-bearing ligands (Williams, 1953). The trivalent metals form even stronger bonds and more ionic in character than the divalent metals. This means that many trace metals will be significantly affected by the presence of competing cations in solution.

4.4. Metal assimilation

One obvious question that arises from this study is discriminating between metal cations adsorbed versus assimilated. In the case of Cd, it can substitute for Zn in the enzyme carbonic-anhydrase, which is used in inorganic carbon acquisition (Morel et al., 1994), and some Cd-specific forms of that enzyme have also been shown to exist (Lane et al., 2005). With regards to toxicity, based on minimal Cd isotope fractionation and its nutrient-like behavior in seawater, Horner et al. (2013) speculated that Cd is mistakenly imported with other divalent cations and subsequently managed by its binding to the cell membrane to prevent damage to the cell. Indeed, the mechanism of Cd management in a number of organisms occurs by binding with cysteine-rich peptides, such as glutathione, phytochelatin, or metallothionein (Grill et al., 1987).

Our adsorption/desorption experiments for Cd(II) show that the process is largely reversible, and hence, surface bound. In other words, Cd is adsorbed to the surface functional groups in the wall surface of the *Synechococcus* cells. As previous studies have shown, after rapid adsorption onto the cell surface groups, some Cd slowly diffuses through the cell wall into the cytoplasm, with the magnitude of absorption increasing with time (González-Dávila, 1995). However, our experimental duration was short, and previous experiments conducted under similar conditions exhibited complete and rapid reversal of adsorption reactions, strongly suggesting that the Cd adsorption was onto cell walls and that Cd was not internally assimilated. For instance, it was observed that the Cd adsorption efficiency onto the gram-negative species *Escherichia coli* (8.9×10^{-5} M Cd, 1.0 g/L (dry weight) bacteria, pH of 3.5) was around 25% after 2 h compared to 30% after 12 h and the process is fully reversible (Yee and Fein, 2001). Fowle and Fein (2000) demonstrated that Cd rapidly adsorbed onto the gram-positive bacteria *Bacillus subtilis* (total 10^{-4} M Cd, of 10 g/L (wet weight) bacteria, pH = 4) and reached a steady-state extent of adsorption of 34% within 2 h, then the adsorption remained constant for the following 22 h (and up to 80 h). Chang et al. (1997) described the reversibility of *P. aeruginosa* PU21 initially containing 1.5×10^{-3} M Cd and 1–2 g/L cell (wet weight) at pH 6.0 by repeating the adsorption/desorption cycles 4 times, and found that the recovery efficiency of Cd was around 70–80%. Cd loss was attributed to the loss of 30–45% of the suspended cells after 4 adsorption/desorption cycles.

4.5. Implications for marine metal cycling

This study confirms a hypothesis proposed thirty years ago, that picoplankton are ideally suited to scavenge trace metals from seawater owing to their rapid growth rates and large surface area-to-volume ratios (Fisher, 1985). Heterotrophic bacteria and viruses are even more abundant and have larger surface area:volume ratios (Cochlan et al., 1993), so they are also likely to play a significant role in trace metal sequestration. Here we demonstrate that cell wall composition/charge characteristics of phytoplanktonic *Synechococcus* are also critically important to the metal binding process. While many previous studies on trace metal cycling in the water column have considered depletion in Redfield-like metal proportions (Sigg, 1994), we confirm that simple adsorption by phytoplankton has the potential to be a significant mechanism in the removal of metals from seawater (Tovar-Sanchez et al., 2003).

The above discussion has obvious implications for the transfer of Cd from the water column to the bottom sediments, and ultimately, its incorporation into the rock record. However, a number of unknowns remain that preclude an accurate estimation of how effective plankton are as Cd fluxes to the seafloor. First, it presently remains unclear how much of the particulate Cd in the water

column (i.e., 10% of the total Cd) is associated with phytoplankton, and what fraction of the dissolved organic complexes are the degradation products of lysed cells. Second, longer-term experimental studies are required to discriminate between the amount of Cd adsorbed to the cellular surfaces versus the amount of Cd assimilated to fulfill biological functions. The use of, for example, metal isotope adsorption/assimilation studies may help to address this issue (Wasylenki et al., 2007; Zerkle et al., 2011). Third, Cd exhibits nutrient-like behavior in the water column (Bruland and Lohan, 2006; Biller and Bruland, 2013), indicating that grazing and mineralization in the water column liberates much of the sorbed Cd. The next step is to unravel what fraction of the cyanobacteria-bound Cd reaches the seafloor, thus necessitating measurements of Cd sedimentation rates, speciation determination of the organic versus inorganic Cd phases in the bottom sediments, and the use of biomarkers to assess what fraction of organically-bound Cd originated as cyanobacteria.

While our discussion has been focused on Cd due to its frequent use in biosorption experiments with which we wanted to compare our results, the ability of phytoplankton to adsorb metals from surface seawater extends to the entire spectrum of elements. In this regard, our future efforts will be to experimentally determine the adsorption of different trace metals, both those with nutritional needs and those that are toxic, to *Synechococcus* and other marine phytoplankton.

ACKNOWLEDGMENTS

The authors would like to thank the following for their assistance with the various analyses: FTIR in the Department of Chemistry Analytical and Instrumentation Laboratory, University of Alberta (Wayne Moffat); ICP-MS was performed in the Department of Renewable Resources Natural Resources Analytical Laboratory (Xin Zhang); zeta potential measurement was performed in the Department of Chemical and Materials Engineering Laboratory (Jim Skwarok); and SEM and TEM analysis in the Department of Biological Sciences (Arlene Oatway). This work was supported by a Natural Science and Engineering Research Council grant to K.O.K., G.W.O. and D.S.A., and S.V.L. from the region of Brittany and LabexMER.

APPENDIX A. SUPPLEMENTARY DATA

Supplementary data associated with this article can be found, in the online version, at http://dx.doi.org/10.1016/j.gca.2015.07.033.

REFERENCES

Acharya C. and Apte S. K. (2013) Insights into the interactions of cyanobacteria with uranium. *Photosynth. Res.* **118**, 83–94.

Acharya C., Joseph D. and Apte S. (2009) Uranium sequestration by a marine cyanobacterium, *Synechococcus elongatus* strain BDU/75042. *Bioresour. Technol.* **100**, 2176–2181.

Acharya C., Chandwadkar P. and Apte S. (2012) Interaction of uranium with a filamentous, heterocystous, nitrogen-fixing cyanobacterium, *Anabaena torulosa*. *Bioresour. Technol.* **116**, 290–294.

Acharya C., Chandwadkar P., Joseph D. and Apte S. (2013) Uranium (VI) recovery from saline environment by a marine unicellular cyanobacterium, *Synechococcus elongatus*. *J. Radioanal. Nucl. Chem.* **295**, 845–850.

Ahimou F., Paquot M., Jacques P., Thonart P. and Rouxhet P. G. (2001) Influence of electrical properties on the evaluation of the surface hydrophobicity of *Bacillus subtilis*. *J. Microbiol. Methods* **45**, 119–126.

Ahner B. A. and Morel F. M. (1995) Phytochelatin production in marine algae. 2. Induction by various metals. *Limnol. Oceanogr.* **40**, 658–665.

Ahner B. A., Lee J. G., Price N. M. and Morel F. M. (1998) Phytochelatin concentrations in the equatorial Pacific. *Deep Sea Res. Part I* **45**, 1779–1796.

Alessi D. S. and Fein J. B. (2010) Cadmium adsorption to mixtures of soil components: testing the component additivity approach. *Chem. Geol.* **270**, 186–195.

Alessi D. S., Henderson J. M. and Fein J. B. (2010) Experimental measurement of monovalent cation adsorption onto *Bacillus subtilis* cells. *Geomicrobiol J.* **27**, 464–472.

Baes C. F. and Mesmer R. E. (1976) Hydrolysis of Cations. Wiley Interscience Publication, New York.

Baker M. G., Lalonde S. V., Konhauser K. O. and Foght J. M. (2010) Role of extracellular polymeric substances in the surface chemical reactivity of *Hymenobacter aerophilus*, a psychrotolerant bacterium. *Appl. Environ. Microbiol.* **76**, 102–109.

Benning L. G., Phoenix V. R., Yee N. and Konhauser K. O. (2004) The dynamics of cyanobacterial silicification: an infrared micro-spectroscopic investigation. *Geochim. Cosmochim. Acta* **68**, 743–757.

Bethke C. M. and Brady P. V. (2000) How the Kd approach undermines ground water cleanup. *Ground Water* **38**, 435–443.

Biller D. V. and Bruland K. W. (2013) Sources and distributions of Mn, Fe Co, Ni, Cu, Zn, and Cd relative to macronutrients along the central California coast during the spring and summer upwelling season. *Mar. Chem.* **155**, 50–70.

Borrok D., Fein J. B. and Kulpa C. F. (2004a) Proton and Cd adsorption onto natural bacterial consortia: testing universal adsorption behavior. *Geochim. Cosmochim. Acta* **68**, 3231–3238.

Borrok D. M., Fein J. B. and Kulpa C. F. (2004b) Cd and proton adsorption onto bacterial consortia grown from industrial wastes and contaminated geologic settings. *Environ. Sci. Technol.* **38**, 5656–5664.

Borrok D., Turner B. F. and Fein J. B. (2005) A universal surface complexation framework for modeling proton binding onto bacterial surfaces in geologic settings. *Am. J. Sci.* **305**, 826–853.

Brahamsha B. (1996) An abundant cell-surface polypeptide is required for swimming by the nonflagellated marine cyanobacterium *Synechococcus*. *Proc. Natl. Acad. Sci. U.S.A.* **93**, 6504–6509.

Bruland K. W. (1992) Complexation of cadmium by natural organic ligands in the central North Pacific. *Limnol. Oceanogr.* **37**, 1008–1017.

Bruland K. and Lohan M. (2006). *Controls of trace metals in seawater*. , pp. 23–47. The Oceans and Marine Geochemistry.

Byrne R. H., Kump L. and Cantrell K. (1988) The influence of temperature and pH on trace metal speciation in seawater. *Mar. Chem.* **25**, 163–181.

Cao Y. Y., Wei X., Cai P., Huang Q. Y., Rong X. M. and Liang W. (2011) Preferential adsorption of extracellular polymeric substances from bacteria on clay minerals and iron oxide. *Colloids Surf. B Biointerfaces* **83**, 122–127.

Chang J. S., Law R. and Chang C. C. (1997) Biosorption of lead, copper and cadmium by biomass of *Pseudomonas aeruginosa* PU21. *Water Res.* **31**, 1651–1658.

Claessens J., Behrends T. and Van Cappellen P. (2004) What do acid-base titrations of live bacteria tell us? A preliminary assessment. *Aquat. Sci.* **66**, 19–26.

Clarke W. A., Konhauser K. O., Thomas J. C. and Bottrell S. H. (1997) Ferric hydroxide and ferric hydroxysulfate precipitation by bacteria in an acid mine drainage lagoon. *FEMS Microbiol. Rev.* **20**, 351–361.

Cochlan W. P., Wikner J., Steward G. F., Smith D. C. and Azam F. (1993) Spatial distribution of viruses, bacteria and chlorophyll a in neritic, oceanic and estuarine environments. *Mar. Ecol. Prog. Ser.* **92**, 77.

Cox J. S., Smith D. S., Warren L. A. and Ferris F. G. (1999) Characterizing heterogeneous bacterial surface functional groups using discrete affinity spectra for proton binding. *Environ. Sci. Technol.* **33**, 4514–4521.

Danielsson L. G., Magnusson B. and Westerlund S. (1985) Cadmium, copper, iron, nickel and zinc in the north-east Atlantic Ocean. *Mar. Chem.* **17**, 23–41.

de Baar H. J., Saager P. M., Nolting R. F. and van der Meer J. (1994) Cadmium versus phosphate in the world ocean. *Mar. Chem.* **46**, 261–281.

Dittrich M. and Sibler S. (2005) Cell surface groups of two picocyanobacteria strains studied by zeta potential investigations, potentiometric titration, and infrared spectroscopy. *J. Colloid Interface Sci.* **286**, 487–494.

Dittrich M. and Sibler S. (2006) Influence of H^+ and calcium ions on surface functional groups of *Synechococcus* PCC 7942 cells. *Langmuir* **22**, 5435–5442.

Dupont C. L. and Ahner B. A. (2005) Effects of copper, cadmium, and zinc on the production and exudation of thiols by *Emiliania huxleyi*. *Limnol. Oceanogr.* **50**, 508–515.

Fattom A. and Shilo M. (1984) Hydrophobicity as an adhesion mechanism of benthic cyanobacteria. *Appl. Environ. Microbiol.* **47**, 135–143.

Fein J. B. (2006) Thermodynamic modeling of metal adsorption onto bacterial cell walls: current challenges. *Adv. Agron.* **90**, 179–202.

Fein J. B., Daughney C. J., Yee N. and Davis T. A. (1997) A chemical equilibrium model for metal adsorption onto bacterial surfaces. *Geochim. Cosmochim. Acta* **61**, 3319–3328.

Fein J. B., Boily J.-F., Yee N., Gorman-Lewis D. and Turner B. F. (2005) Potentiometric titrations of *Bacillus subtilis* cells to low pH and a comparison of modeling approaches. *Geochim. Cosmochim. Acta* **69**, 1123–1132.

Fisher N. (1985) Accumulation of metals by marine picoplankton. *Mar. Biol.* **87**, 137–142.

Flombaum P., Gallegos J. L., Gordillo R. A., Rincón J., Zabala L. L., Jiao N., Karl D. M., Li W. K., Lomas M. W. and Veneziano D. (2013) Present and future global distributions of the marine Cyanobacteria *Prochlorococcus* and *Synechococcus*. *Proc. Natl. Acad. Sci. U.S.A.* **110**, 9824–9829.

Fowle D. A. and Fein J. B. (2000) Experimental measurements of the reversibility of metal–bacteria adsorption reactions. *Chem. Geol.* **168**, 27–36.

González-Dávila M. (1995) The role of phytoplankton cells on the control of heavy metal concentration in seawater. *Mar. Chem.* **48**, 215–236.

González-Dávila M., Santana-Casiano J. M., Perez-Pena J. and Millero F. J. (1995) Binding of Cu (II) to the surface and exudates of the alga *Dunaliella tertiolecta* in seawater. *Environ. Sci. Technol.* **29**, 289–301.

Grill E., Winnacker E.-L. and Zenk M. H. (1987) Phytochelatins, a class of heavy-metal-binding peptides from plants, are functionally analogous to metallothioneins. *Proc. Natl. Acad. Sci. U.S.A.* **84**, 439–443.

Haas J. R., Dichristina T. J. and Wade, Jr, R. (2001) Thermodynamics of U (VI) sorption onto *Shewanella putrefaciens*. *Chem. Geol.* **180**, 33–54.

Hadjoudja S., Deluchat V. and Baudu M. (2010) Cell surface characterisation of *Microcystis aeruginosa* and *Chlorella vulgaris*. *J. Colloid Interface Sci.* **342**, 293–299.

Herbelin A. L. and Westall J. C. (1999) FITEQL 4.0: A computer program for determination of chemical equilibrium constants from experimental data.

Horner T. J., Lee R. B., Henderson G. M. and Rickaby R. E. (2013) Nonspecific uptake and homeostasis drive the oceanic cadmium cycle. *Proc. Natl. Acad. Sci. U.S.A.* **110**, 2500–2505.

Jiang W., Saxena A., Song B., Ward B. B., Beveridge T. J. and Myneni S. C. (2004) Elucidation of functional groups on gram-positive and gram-negative bacterial surfaces using infrared spectroscopy. *Langmuir* **20**, 11433–11442.

Johnson K., Szymanowski J., Borrok D., Huynh T. and Fein J. (2007) Proton and metal adsorption onto bacterial consortia: stability constants for metal–bacterial surface complexes. *Chem. Geol.* **239**, 13–26.

Kapetas L., Ngwenya B. T., Macdonald A. M. and Elphick S. C. (2011) Kinetics of bacterial potentiometric titrations: the effect of equilibration time on buffering capacity of *Pantoea agglomerans* suspensions. *J. Colloid Interface Sci.* **359**, 481–486.

Kenney J. P. L. and Fein J. B. (2011) Cell wall reactivity of acidophilic and alkaliphilic bacteria determined by potentiometric titrations and cd adsorption experiments. *Environ. Sci. Technol.* **45**, 4446–4452.

Konhauser K. O. (2007) *Introduction to Geomicrobiology*. Blackwell Publishing, Oxford.

Konhauser K. O., Fisher Q. J., Fyfe W. S., Longstaffe F. J. and Powell M. A. (1998) Authigenic mineralization and detrital clay binding by freshwater biofilms: the Brahmani River, India. *Geomicrobiol. J.* **15**, 209–222.

Lalonde S. V., Amskold L. A., Warren L. A. and Konhauser K. O. (2007) Surface chemical reactivity and metal adsorptive properties of natural cyanobacterial mats from an alkaline hydrothermal spring, Yellowstone National Park. *Chem. Geol.* **243**, 36–52.

Lalonde S. V., Smith D. S., Owttrim G. W. and Konhauser K. O. (2008a) Acid–base properties of cyanobacterial surfaces. II: silica as a chemical stressor influencing cell surface reactivity. *Geochim. Cosmochim. Acta* **72**, 1269–1280.

Lalonde S. V., Smith D. S., Owttrim G. W. and Konhauser K. O. (2008b) Acid–base properties of cyanobacterial surfaces I: influences of growth phase and nitrogen metabolism on cell surface reactivity. *Geochim. Cosmochim. Acta* **72**, 1257–1268.

Lalonde S. V., Dafoe L. T., Pemberton S. G., Gingras M. K. and Konhauser K. O. (2010) Investigating the geochemical impact of burrowing animals: Proton and cadmium adsorption onto the mucus lining of *Terebellid* polychaete worms. *Chem. Geol.* **271**, 44–51.

Lane T. W., Saito M. A., George G. N., Pickering I. J., Prince R. C. and Morel F. M. (2005) Biochemistry: a cadmium enzyme from a marine diatom. *Nature* **435**, 42.

Ledin M., Pedersen K. and Allard B. (1997) Effects of pH and ionic strength on the adsorption of Cs, Sr, Eu, Zn, Cd and Hg by *Pseudomonas putida*. *Water Air Soil Pollut.* **93**, 367–381.

Leone L., Ferri D., Manfredi C., Persson P., Shchukarev A., Sjöberg S. and Loring J. (2007) Modeling the acid-base properties of bacterial surfaces: a combined spectroscopic and potentiometric study of the gram-positive bacterium *Bacillus subtilis*. *Environ. Sci. Technol.* **41**, 6465–6471.

Mart L., Rützel H., Klahre P., Sipos L., Platzek U., Valenta P. and Nürnberg H. (1982) Comparative studies on the distribution of

heavy metals in the oceans and coastal waters. *Sci. Total Environ.* **26**, 1–17.

Martinez R. E., Pedersen K. and Ferris F. G. (2004) Cadmium complexation by bacteriogenic iron oxides from a subterranean environment. *J. Colloid Interface Sci.* **275**, 82–89.

Mishra B., Boyanov M., Bunker B. A., Kelly S. D., Kemner K. M. and Fein J. B. (2010) High-and low-affinity binding sites for Cd on the bacterial cell walls of *Bacillus subtilis* and *Shewanella oneidensis*. *Geochim. Cosmochim. Acta* **74**, 4219–4233.

Morel F., Reinfelder J., Roberts S., Chamberlain C., Lee J. and Yee D. (1994) Zinc and carbon co-limitation of marine phytoplankton. *Nature* **369**, 740–742.

Mozes N., Léonard A. and Rouxhet P. G. (1988) On the relations between the elemental surface composition of yeasts and bacteria and their charge and hydrophobicity. *Biochim. Biophys. Acta* **945**, 324–334.

Neilands J. (1995) Siderophores: structure and function of microbial iron transport compounds. *J. Biol. Chem.* **270**, 26723–26726.

Ntalikwa J. W. (2007) Determination of surface charge density of α-alumina by acid–base titration. *Bull. Chem. Soc. Ethiop.* **21**, 117–128.

Ojeda J. J., Romero-González M. E., Bachmann R. T., Edyvean R. G. and Banwart S. A. (2008) Characterization of the cell surface and cell wall chemistry of drinking water bacteria by combining XPS, FTIR spectroscopy, modeling, and potentiometric titrations. *Langmuir* **24**, 4032–4040.

Ong Y.-L., Razatos A., Georgiou G. and Sharma M. M. (1999) Adhesion forces between *E. coli* bacteria and biomaterial surfaces. *Langmuir* **15**, 2719–2725.

Pai S. C. and Chen H. Y. (1994) Vertical distribution of cadmium in marginal seas of the western Pacific Ocean. *Mar. Chem.* **47**, 81–91.

Peng Y., Wu P. Y. and Siesler H. W. (2003) Two-dimensional/ATR infrared correlation spectroscopic study on water diffusion in a poly(-caprolactone) matrix. *Biomacromolecules* **4**, 1041–1044.

Petersen K., Kristensen E. and Bjerregaard P. (1998) Influence of bioturbating animals on flux of cadmium into estuarine sediment. *Mar. Environ. Res.* **45**, 403–415.

Petrash D. A., Lalonde S. V., Gingras M. K. and Konhauser K. O. (2011) A surrogate approach to studying the chemical reactivity of burrow mucous linings in marine sediments. *Palaios* **26**, 594–600.

Phoenix V. R., Adams D. G. and Konhauser K. O. (2000) Cyanobacterial viability during hydrothermal biomineralisation. *Chem. Geol.* **169**, 329–338.

Phoenix V. R., Martinez R. E., Konhauser K. O. and Ferris F. G. (2002) Characterization and implications of the cell surface reactivity of *Calothrix* sp. strain KC97. *Appl. Environ. Microbiol.* **68**, 4827–4834.

Pokrovsky O. S., Martinez R., Golubev S., Kompantseva E. and Shirokova L. (2008) Adsorption of metals and protons on *Gloeocapsa* sp. cyanobacteria: a surface speciation approach. *Appl. Geochem.* **23**, 2574–2588.

Sherrell R. M. and Boyle E. A. (1992) The trace metal composition of suspended particles in the oceanic water column near Bermuda. *Earth Planet. Sci. Lett.* **111**, 155–174.

Sigg L. (1994) *Regulation of trace elements in lakes: the role of sedimentation.* , pp. 175–195.

Stevens S. E. and Porter R. D. (1980) Transformation in *Agmenellum quadruplicatum*. *Proc. Natl. Acad. Sci. U.S.A.* **77**, 6052–6056.

Stevens S. and Van Baalen C. (1973) Characteristics of nitrate reduction in a mutant of the blue-green alga *Agmenellum quadruplicatum*. *Plant Physiol.* **51**, 350–356.

Stipp S. L., Parks G. A., Nordstrom D. K. and Leckie J. O. (1993) Solubility-product constant and thermodynamic properties for synthetic otavite, $CdCO_3$ (s), and aqueous association constants for the Cd(II)–CO_2–H_2O system. *Geochim. Cosmochim. Acta* **57**, 2699–2713.

Tovar-Sanchez A., Sañudo-Wilhelmy S. A., Garcia-Vargas M., Weaver R. S., Popels L. C. and Hutchins D. A. (2003) A trace metal clean reagent to remove surface-bound iron from marine phytoplankton. *Mar. Chem.* **82**, 91–99.

Ueshima M., Ginn B. R., Haack E. A., Szymanowski J. E. S. and Fein J. B. (2008) Cd adsorption onto *Pseudomonas putida* in the presence and absence of extracellular polymeric substances. *Geochim. Cosmochim. Acta* **72**, 5885–5895.

Urrutia M. M. and Beveridge T. J. (1993) Remobilization of heavy metals retained as oxyhydroxides or silicates by *Bacillus subtilis* cells. *Appl. Environ. Microbiol.* **59**, 4323–4329.

Van Loosdrecht M., Lyklema J., Norde W., Schraa G. and Zehnder A. (1987) The role of bacterial cell wall hydrophobicity in adhesion. *Appl. Environ. Microbiol.* **53**, 1893–1897.

Wasylenki L., Anbar A., Liermann L., Mathur R., Gordon G. and Brantley S. (2007) Isotope fractionation during microbial metal uptake measured by MC-ICP-MS. *J. Anal. At. Spectrom.* **22**, 905–910.

Waterbury J. B., Watson S. W., Guillard R. R. and Brand L. E. (1979) Widespread occurrence of a unicellular, marine, planktonic, cyanobacterium. *Nature* **277**, 293–294.

Wei X., Fang L. C., Cai P., Huang Q. Y., Chen H., Liang W. and Rong X. M. (2011) Influence of extracellular polymeric substances (EPS) on Cd adsorption by bacteria. *Environ. Pollut.* **159**, 1369–1374.

Wells M. L., Kozelka P. B. and Bruland K. W. (1998) The complexation of 'dissolved' Cu, Zn, Cd and Pb by soluble and colloidal organic matter in Narragansett Bay, RI. *Mar. Chem.* **62**, 203–217.

Westall J. C. (1982) *FITEQL: A Computer Program for Determination of Chemical Equilibrium Constants from Experimental Data*. Department of Chem. Oregon State Univ.

Williams R. J. (1953) Metal ions in biological systems. *Biol. Rev. Camb. Philos. Soc.* **28**, 381–412.

Worden A. Z., Nolan J. K. and Palenik B. (2004) Assessing the dynamics and ecology of marine picophytoplankton: the importance of the eukaryotic component. *Limnol. Oceanogr.* **49**, 168–179.

Yee N. and Fein J. (2001) Cd adsorption onto bacterial surfaces: a universal adsorption edge? *Geochim. Cosmochim. Acta* **65**, 2037–2042.

Yee N., Benning L. G., Phoenix V. R. and Ferris F. G. (2004) Characterization of metal–cyanobacteria sorption reactions: a combined macroscopic and infrared spectroscopic investigation. *Environ. Sci. Technol.* **38**, 775–782.

Zerkle A., Scheiderich K., Maresca J., Liermann L. and Brantley S. (2011) Molybdenum isotope fractionation by cyanobacterial assimilation during nitrate utilization and N_2fixation. *Geobiology* **9**, 94–106.

Zirino A. and Yamamoto S. (1972) A pH-dependent model for the chemical speciation of copper, zinc, cadmium, and lead in seawater. *Limnol. Oceanogr.* **17**, 661–671.

Associate editor: Benjamin Van Mooy